ELSEVIER

Journal of Alloys and Compounds 438 (2007) 88–91

ALLOYS AND COMPOUNDS

www.elsevier.com/locate/jallcom

Structural analysis and ^{57}Fe Mössbauer spectrometry of Zr_6FeSn_2 and related compounds

B.F.O. Costa [a,*], J.M. Greneche [b], D. Fruchart [c], H.V. Alberto [a], N.E. Skryabina [c,d], L.P. Romaka [e], Yu.V. Stadnyk [e]

[a] *Departamento de Física da Universidade de Coimbra, P-3004-516 Coimbra, Portugal*
[b] *Université du Maine, Laboratoire de Physique de l'Etat Condensé, 72085 Le Mans, France*
[c] *Laboratoire de Cristallographie, CNRS, BP 166, F-38042 Grenoble Cedex 9, France*
[d] *Solid State Department, Perm State University, 15 Bukirev St., 614990 Perm, Russia*
[e] *Chemistry Department, I. Franko University, Lviv 29005, Ukraine*

Received 3 July 2006; received in revised form 31 July 2006; accepted 1 August 2006
Available online 18 September 2006

Abstract

Hexagonal compounds of formula Zr_6FeX_2 were prepared and studied by X-ray and neutron diffraction and by ^{57}Fe Mössbauer spectroscopy. The first results indicate that most of the compounds can be prepared mainly as a single phase after at least 5 weeks of annealing at a temperature close to 900 °C. In particular, the hyperfine parameter distributions in Mössbauer spectra reflect the ability to form pure phases.

PACS: 75.40.−s; 71.20.LP

Keywords: Ternary Zr based compounds; Crystal structure; Mössbauer spectroscopy

1. Introduction

The compounds Zr_6FeX_2 and Hf_6FeX_2 belong to a large series of $M'_6M''_{1.5+x}X_{1.5-x}$ with M′ = Ti, Zr, Hf, etc.; M″ = Fe, Co, Ni, etc.; X = Al, Sn, Sb, etc., the structure of which is related to the Fe_2P type (space group $P\bar{6}2m$) [1–5] as seen in Fig. 1. In the unit cell, the M′ atoms occupy the 3f sites at (x, 0, 0) and the 3g sites at (x, 0, 1/2), with x close to 0.245 and 0.603, respectively. The M″ atoms are distributed between two sites: 1b at (0, 0, 1/2) and 2c site at (2/3, 1/3, 0). This later site is randomly shared with the X element. These compounds were found to be interesting materials to store hydrogen [4] since they can absorb more hydrogen than $LaNi_5$, a reference compound. For example, to Zr_6NiAlH_{12} corresponds a ratio $H_{max}/M = 1.5$ (or 1.8 wt%) in contrast with $H_{max}/M = 1.0$ (or 1.4 wt%) for $LaNi_5H_6$ [1].

These ternary compounds present an additional interest since they contain elements such as Al and Sb that are known to form weak bonds with hydrogen, thus leading to increase the equilibrium pressure and consequently to decrease the hydride stability.

Prior to a systematic study of the thermodynamic behaviour of the metal–hydrogen systems, we aim to analyse in detail the local environment associated with the Fe to X atomic distribution. This distribution is possibly one of the main factors controlling the stability of interstitial hydrogen atoms.

A first survey of the compounds Zr_6FeX_2 (X = Sb and Sn) is presented in this work using ^{57}Fe Mössbauer spectrometry. Some of the compounds were also studied by X-ray and neutron diffraction.

2. Experimental

2.1. Synthesis of the samples

The compounds Zr_6TX_2 (T = Fe, Co, X = Sb and Sn) were prepared by melting together the components using an arc furnace for the first series of samples and the HF cold crucible technique for the second series, both under a purified argon atmosphere. In the case of samples with Al and Sb, an excess of the later elements was added to prevent losses by evaporation. The samples were melted several times and then annealed between 800 and 850 °C in evacuated quartz tubes to ensure homogeneity. The first of the two series of samples was annealed

* Corresponding author. Tel.: +351 239410630; fax: +351 239829158.
E-mail address: benilde@ci.uc.pt (B.F.O. Costa).

0925-8388/$ – see front matter © 2006 Elsevier B.V. All rights reserved.
doi:10.1016/j.jallcom.2006.08.046

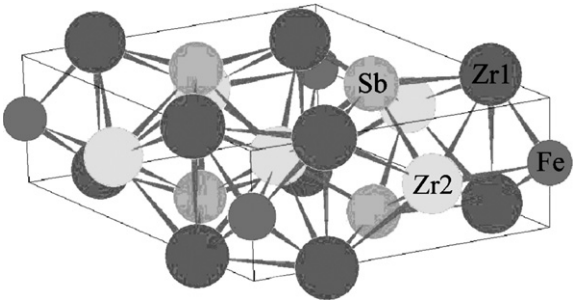

Fig. 1. Crystal structure of Zr_6FeSb_2 (SG $P\bar{6}2m$, $a = 7.756$ Å, $c = 3.658$ Å). Zr1 atoms (3f position with $x = 0.2456$) are represented by dark circles, Zr2 atoms (3g position with $x = 0.6034$) are represented by clear circles, Fe atoms (1b position) are represented by small circles and Sb atoms (2c position) are represented by medium dark circles.

for 2 weeks while the second series of samples being annealed for 5 weeks under inert gas atmosphere.

2.2. X-ray diffraction analysis

Systematic X-ray analyses were performed using a transmission Siemens D5000 diffractometer (λCu Kα target) to confirm that the phases were mainly Zr_6FeX_2 type compounds. In some cases, a small fraction of impurities was detected, particularly in the samples annealed for 2 weeks only. This observation led us to decide to prepare samples with longer annealing times. However, a clear identification of the extra phases was not made easy owing to the large number of diffraction peaks of the main compound. A typical X-ray diffraction pattern is shown in Fig. 2, corresponding to a Zr_6FeSb_2 sample of the long time annealed series. There was noticed a small change in the cell parameters from the first series of batches to the second ones since the *c*/*a* ratio reduces from 0.474 to 0.472 for the parent Zr_6TSb_2 samples with T = Fe, Co. The final cell parameters of the longer time annealed samples are found close to those already reported in refs. [1,5]. The cell parameter values are listed in Table 1. Such a reduction of the *c*/*a* ratio observed between the 2 and 5 weeks annealed samples results from a decrease of the *c* cell parameter while the *a* cell parameter increases, however slightly. This change should be the result of atom reordering, e.g. better distributions of Fe and Sb onto the 1b and 2c sites, respectively. Effectively both atoms occupy similar sites formed with Zr1 and Zr2 sites (3f and 3g sites, respectively). The corresponding coordination polyhedron called a tetrakaïdecahedron, is formed from a regular triangular prism of six Zr1 (Zr2) neighbours and three Zr2 (Zr1) atoms capping the rectangular faces of the prism, for a total of nine Zr-neighbours. However, if the Zr-coordination looks very similar, the Fe–Zr and Sb–Zr distances are different. For Zr_6FeSb_2, the interatomic

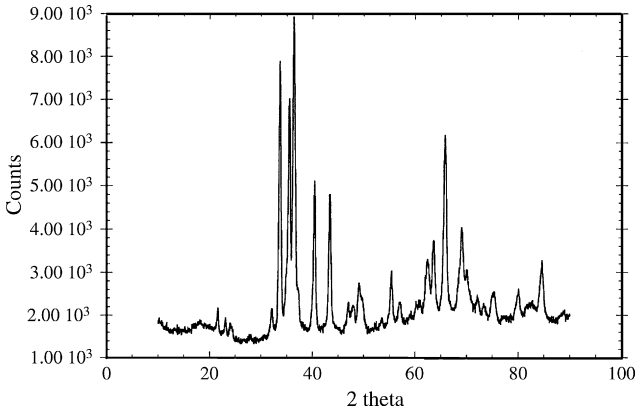

Fig. 2. X-ray diffraction pattern recorded on the Zr_6FeSb_2 compounds as annealed for 5 weeks between 800 and 850 °C (nominal starting composition was Zr_7FeSb_2).

Table 1
Cell parameters of the long time annealed Zr_6MX_2 compounds with M = Fe, Co, X = Sn, Sb

Sample	*a* (Å)	*c* (Å)
Zr_6FeSn_2	7.994	3.465
Zr_6FeSb_2	7.756	3.658
Zr_6CoSn_2	7.973	3.450
Zr_6CoSb_2	7.758	3.647

distances are, respectively of:

2c	6 × Sb–Zr1	2.98 Å	3 × Sb–Zr2	2.99 Å
1b	6 × Fe–Zr2	2.64 Å	3 × Fe–Zr1	3.08 Å

Thus, some Sb atoms occupying the 1b site will lead to increase (decrease) the *a* (*c*) cell parameter, correspondingly. The distribution of Fe and Sb onto the 1b and 2c sites will be discussed later on the basis of Mössbauer data. This can explain that from ^{57}Fe Mössbauer spectrometry, two different iron spectra are observed in a proportion close to 50/50, however corresponding to a relative preferential 2c site occupation by antimony. However, the crystal structure refinements indicate a good agreement factor for the ordered repartition, R_B being 3.3%.

2.3. Neutron diffraction analysis of the Zr_6FeX_2 (X = Sb and Sn)

Neutron diffraction patterns were recorded using the D1A diffractometer setting at the Institute Laue Langevin, Grenoble, France. The diffraction patterns were recorded at room temperature, the neutron wavelength being λ = 1.991 Å. A typical pattern is represented in Fig. 3, corresponding to the Zr_6FeX_2 compound after 5 weeks annealing time. Several minor lines of the pattern corresponding to impurities, have been marked by black dots. Different binary phases (e.g. FeSb, $FeSb_2$, $ZrFe_2$, Zr_2Fe, ...) were checked for identification of the extra lines. The best agreement indicates the phase is more probably the tetragonal $ZrFe_2$ with the $CuAl_2$ type structure. Elements like Sn, Sb, ... can be substitutionally incorporated since a similar structure also exists with the $FeSn_2$ formula. This later type of phase is not known to react appreciably with hydrogen. So in all forthcoming studies, hydrogen uptake is attributed only to the main phase of the Zr_6FeX_2 type of structure.

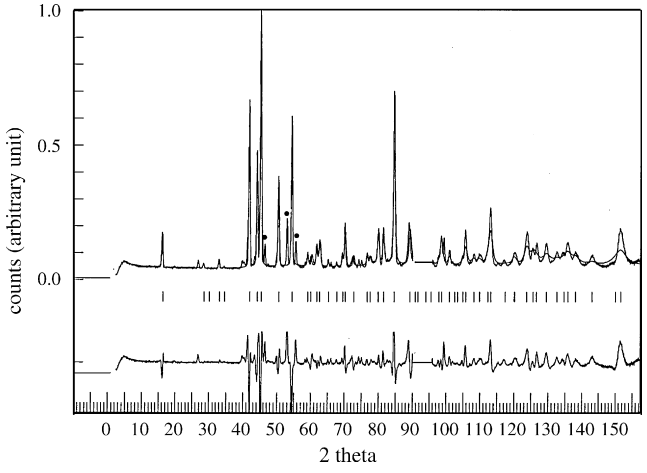

Fig. 3. Neutron diffraction pattern recorded using the D1A diffractometer (ILL, Grenoble) at room temperature with λ = 1.911 Å on the Zr_6FeSb_2 compounds after annealing for 5 weeks between 800 and 850 °C (nominal starting composition was Zr_7FeSb_2). Three dots indicate the lines corresponding to a small fraction of impurities (see text). Ticks indicate the Bragg lines of the main compound. A difference diagram Obs-Calc is plotted in the lower part of the figure. The final R_{Bragg} factor for the main phase is 0.033.

2.4. ^{57}Fe Mössbauer spectrometry

Mössbauer spectrometry was used to probe the local atomic structure of the compounds. ^{57}Fe Mössbauer spectra were recorded at 300, 77 and 4.2 K in transmission mode with a spectrometer operating in a conventional constant acceleration mode and using a liquid He bath cryostat. A ^{57}Co source diffused into a Rh matrix with a strength of ≈50 mCi was used. The spectra were analysed using a set of Lorentzian lines as fitting functions. The values of the isomer shift (IS) are given relative to that of α-Fe.

3. Results and discussion

The Mössbauer spectra show only pure quadrupolar hyperfine structures, as illustrated in Figs. 4 and 5. In the case of Sn containing samples (Fig. 4), one can unambiguously observe the presence of three lines suggesting two quadrupolar components, which can be fitted according two different ways. Indeed, four lorentzian lines can be adjusted either coupling the two most external and two internal lines, or coupling together crossed lines. Such descriptions lead to two quadrupolar components with either two similar isomer shifts and two different quadrupole splittings, or two different isomer shifts and two similar quadrupole splittings. According to both the values of isomer shifts and the temperature dependence of some hyperfine parameters and X-ray patterns, we have chosen the second hypothesis as Sb (and Sn) prefers occupy the 2c site. In the case of Zr_6FeSb, one observes from Fig. 5 an asymmetrical quadrupolar doublet with broadened lines. The presence of preferential orientation has been confirmed by rotating the sample respect to the γ-beam direction and consequently, the hyperfine structure was described by means of two asymmetrical quadrupolar doublet. The hyperfine parameters are listed in Table 2, for the indicated samples at different temperatures. From both diffraction and Mössbauer data, the crystallographic data indicates the presence of only one Fe site, the 1b site, as the 2c site is mainly occupied by the Sb atoms.

From literature on the $ZrFe_2$ type materials, there are two sites in crystalline compounds with isomer shifts about −0.07 and −0.18 mm/s at 77 and 293 K, respectively [6]. In both cases, the spectra are magnetic and the hyperfine fields are about

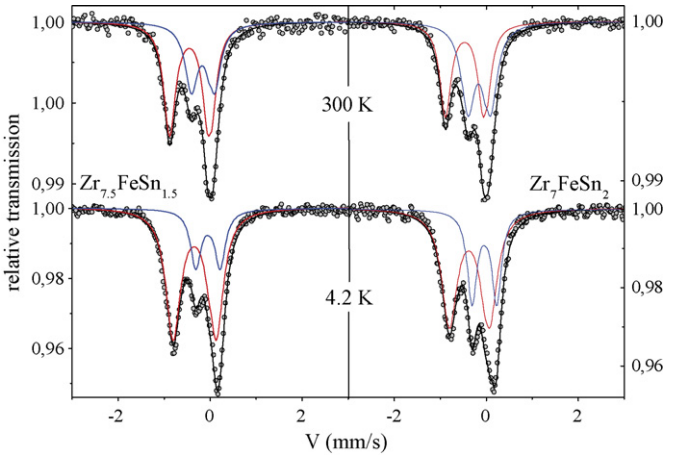

Fig. 4. ^{57}Fe Mössbauer spectra recorded at 300 and at 4.2 K on Sn containing samples.

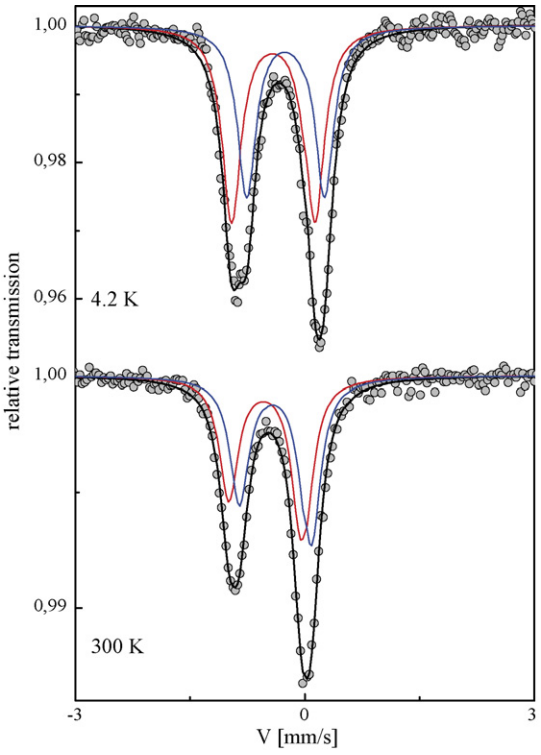

Fig. 5. ^{57}Fe Mössbauer spectra recorded at 300 and at 4.2 K on Sb containing samples.

20.0 T. For disordered alloys [7], the authors distinguish between mechanical ground alloys (MG) and mechanically alloyed (MA) samples. In both cases, they obtained a magnetic spectrum at 77 K with an hyperfine fied of 17.6 T and isomer shifts of −0.01 and 0.04 mm/s in the case of MG and MA, respectively. At 293 K, the magnetic field disappears and the resulting quadrupolar doublets have isomer shifts of −0.16 and −0.13 mm/s for MG

Table 2
Mössbauer hyperfine parameters obtained from the fits to the spectra of Figs. 4 and 5

Sample	IS ± 0.02 (mm/s)	QS ± 0.02 (mm/s)	Γ ± 0.02(mm/s)	%(±4)
Zr_6FeSn_2				
300 K	−0.36	0.83	0.30	48
	−0.04	0.46	0.34	52
4.2 K	−0.24	0.84	0.41	67
	0.09	0.51	0.26	33
$Zr_{7.5}FeSn_{1.5}$				
300 K	−0.34	0.85	0.51	61
	0.01	0.47	0.34	39
4.2 K	−0.21	0.91	0.39	76
	0.02	0.51	0.28	24
Zr_6FeSb_2				
300 K	−0.39	0.95	0.30	49
	−0.27	0.51	0.30	51
4.2 K	−0.27	1.06	0.30	54
	−0.12	0.99	0.29	46

IS, QS, Γ and % correspond to isomer shift, quadrupolar splitting, line width at half-height and the relative absorption areas, respectively; the isomer shift is quoted to that of α-Fe at 300 K.

and MA, respectively. In the case of Zr-rich amorphous alloys prepared by melt spinning of the same system [8], there is a quadrupolar doublet with a mean isomer shift of −0.25 mm/s at 300 K and for crystallised alloys the obtained doublet has a mean isomer shift of −0.14 mm/s at 300 K.

For the Fe–Sb system [9], the isomer shift decreases from 0.54 to 0.46 mm/s for $Fe_{1.14}$ Sb with the increase in temperature from 6 to 200 K, while the hyperfine field decreases from 11 to 5 T. With an increase of the iron content from 0.14 to 0.35, the isomer shift increases from 0.54 to 0.58 mm/s at 6 K and from 0.14 to 0.35 mm/s at 293 K. In both cases, there is no magnetic hyperfine field. In amorphous Sb containing alloys [10] at 4.2 and 300 K, the isomer shift is rather constant (with the increase of iron content until 60 at% and then it decreases, thus reaching zero for 100 at% Fe. For the content of 60 at% Fe, the isomer shift is 0.4 mm/s. At 77 K in the case of the Fe–Sn system [11] the isomer shift increases with the increase of Sn content, being 0.03 mm/s for FeSn and 0.73 mm/s for $FeSn_2$.

It is important to emphasize that the Mössbauer spectra obtained at 300, 77 and 4.2 K remain rather similar, but differences occur between samples of the first and of the second series. Samples with Sb and Al elements are of difficult preparation since these elements are very volatile. In addition, the lines are particularly broadened in the case of the Zr_6FeSb_2 sample of the second batch. The difference of the samples comes from the annealing time during preparation for 2 weeks between 800 and 850 °C in the case of the first batch and for 5 weeks in the same range of temperature for the second batch. We can therefore conclude that the observed differences might be due to the presence of parasitic phases and that a very long annealing times, a crucial factor, is needed in order to achieve homogeneous samples. Such a work is currently in progress to understand the atomic distribution on the two sites and the role of further thermal treatment.

Acknowledgements

We wish to acknowledge financial supports from FCT/POCTI, co-financed by the FEDER European Community fund (project POCTI/CTM/40759/2001), from ENK6-CT-2002-00600 the EU- HYSTORY Project “Hydrogen Storage in Hydrides for Safe Energy Systems” and from the French Foreign Office Project ECO-NET no. 08133RA.

References

[1] G.A. Melnyk, D. Fruchart, L.P. Romaka, Yu.V. Stadnyk, R.V. Skolozdra, J. Tobola, J. Alloys Compd. 267 (1998) L1–L3.
[2] V.A. Yartys, H. Fjellvag, B.C. Hauback, J. Alloys Compd. 290 (1999) 157–163.
[3] F. Gingl, K. Yvon, I. Yu Zavaliy, V.A. Yartys, P. Fisher, J. Alloys Compd. 226 (1995) 1–4.
[4] L.G. Akselrud, D. Fruchart, N.D. Koblyuk, O. Isnard, G.A. Melnyk, R.V. Skolozdra, Int. J. Hydrogen Energy 24 (1999) 899–907.
[5] G.A. Melnyk, E. Bauer, R.V. Skolozdra, E. Seidl, J. Alloys Compd. 296 (2000) 235–242.
[6] F. Congiu, M. Bionducci, G. Concas, G. Spano, J. Magn. Magn. Mater. 272–276 (2004) 1123–1125.
[7] G. Concas, F. Congiu, G. Spano, M. Bionducci, J. Magn. Magn. Mater. 279 (2004) 421–428.
[8] M. Ghafari, U. Gonser, H.-G. Wagner, Nucl. Instrum. Methods 199 (1982) 197–201.
[9] R. Kumar, K.S. Harchand, M. Vishwamittar, K. Chandra, P. Jernberg, T. Ericsson, R. Wappling, Phys. Rev. B 32 (1985) 69–75.
[10] C.L. Chien, Gang Xiao, K.M. Unruh, Phys. Rev. B 32 (1985) 5582–5590.
[11] G. Trumpy, E. Booth, C. Djega-Mariadassou, P. Lecocq, Phys. Rev. B 2 (1970) 3477–3490.